AMERICAN SOCIETY FOR MICROBIOLOGY | Clinical Microbiology Reviews®

REVIEW

Caseum: a Niche for *Mycobacterium tuberculosis* Drug-Tolerant Persisters

Jansy P. Sarathy,[a] Véronique Dartois[a]

[a]Center for Discovery and Innovation, Hackensack Meridian School of Medicine at Seton Hall University, Nutley, New Jersey, USA

SUMMARY Caseum, the central necrotic material of tuberculous lesions, is a reservoir of drug-recalcitrant persisting mycobacteria. Caseum is found in closed nodules and in open cavities connecting with an airway. Several commonly accepted characteristics of caseum were established during the preantibiotic era, when autopsies of deceased tuberculosis (TB) patients were common but methodologies were limited. These pioneering studies generated concepts such as acidic pH, low oxygen tension, and paucity of nutrients being the drivers of nonreplication and persistence in caseum. Here we review widely accepted beliefs about the caseum-specific stress factors thought to trigger the shift of *Mycobacterium tuberculosis* to drug tolerance. Our current state of knowledge reveals that *M. tuberculosis* is faced with a lipid-rich diet rather than nutrient deprivation in caseum. Variable caseum pH is seen across lesions, possibly transiently acidic in young lesions but overall near neutral in most mature lesions. Oxygen tension is low in the avascular caseum of closed nodules and high at the cavity surface, and a gradient of decreasing oxygen tension likely forms toward the cavity wall. Since caseum is largely made of infected and necrotized macrophages filled with lipid droplets, the microenvironmental conditions encountered by *M. tuberculosis* in foamy macrophages and in caseum bear many similarities. While there remain a few knowledge gaps, these findings constitute a solid starting point to develop high-throughput drug discovery assays that combine the right balance of oxygen tension, pH, lipid abundance, and lipid species to model the profound drug tolerance of *M. tuberculosis* in caseum.

KEYWORDS tuberculosis, granuloma, necrosis, caseum, persistence, phenotypic drug resistance, intracellular lipophilic inclusions, hypoxia, foamy macrophages

Citation Sarathy JP, Dartois V. 2020. Caseum: a niche for *Mycobacterium tuberculosis* drug-tolerant persisters. Clin Microbiol Rev 33:e00159-19. https://doi.org/10.1128/CMR.00159-19.

Address correspondence to Jansy P. Sarathy, jansy.sarathy@hmh-cdi.org.

Published 1 April 2020

INTRODUCTION

In tuberculosis (TB) disease, complex lesions form in the infected organ. Typical pulmonary TB lesions are closed granulomas that start as fully cellular structures and gradually necrotize from the center outward. As they expand, damaging inflammatory processes may locally erode airways, leading to fusion with the necrotic granuloma and formation of an open cavity filled with granuloma remnants. Cavities may also begin as localized foci of lipid pneumonia in the alveolar space upon reactivation of latent infection. In both closed and open lesions, diverse microniches present the infectious agent, *Mycobacterium tuberculosis*, with a variety of environmental conditions to which it must adapt to thrive and/or survive. Caseous necrosis is a hallmark of pulmonary TB pathology. The soft necrotic debris that accumulates in the center of TB granulomas resembles cheese, earning its Latin name, "caseum." The prevailing hypothesis is that the intracaseum *M. tuberculosis* subpopulation (here referred to as "caseum *M. tuberculosis*") contributes to the persistent nature of TB infection in humans and the need for prolonged chemotherapeutic intervention. The proportion of adults with pulmonary TB who have cavitary pathology at the time of diagnosis ranges from 40 to 87% (1). In patients with uncomplicated drug-susceptible TB, a minimum of 6 months of combination therapy with up to four antibiotics is required to optimize the chances of cure (2). The caseous foci of necrotic granulomas and cavities are reservoirs of extracellular bacilli that are recalcitrant to antibiotic treatment (3–6). Direct comparisons between treatment efficacy in TB-infected C3HeB/FeJ (Kramnik) mice, which develop caseous pulmonary granulomas, and BALB/c mice, which do not, revealed that the former are much more refractory to antibiotic treatment (7–9). Lesion-centric drug efficacy studies using rabbit and cynomolgus macaque models of TB infection have been useful in highlighting (i) higher bacterial burden, (ii) deficiency in self-sterilization, and (iii) limited drug-mediated sterilization of caseous granulomas and cavities compared to cellular lesions without a necrotic core (10–12).

Persistence of caseum *M. tuberculosis* is caused by a set of metabolic and physiologic adaptations leading to replication arrest. Using an *ex vivo* assay designed to measure the activity of anti-TB drugs against *M. tuberculosis* present in cavity caseum from infected rabbits, we have shown that this subpopulation exists in a viable but nonreplicating state and exhibits extreme drug tolerance to many 1st- and 2nd-line drugs (13). This problem of phenotypic drug resistance is further compounded by suboptimal drug distribution in the nonvascularized caseous core of necrotic lesions, potentially creating pockets of subinhibitory drug concentrations and *de facto* monotherapy (9, 14, 15). Thus, both pharmacodynamic (drug potency) and pharmacokinetic (drug concentration) factors join forces to increase the chances of treatment failure, relapse, and emergence of drug resistance (16, 17).

In this review, we focus on the progression of necrotic granulomas and the specific metabolic and morphological characteristics of nonreplicating persistent *M. tuberculosis* in caseum. Over the years, scientists have suggested and explored numerous environmental stress factors in the caseous foci. We review four of these factors and their role in triggering *M. tuberculosis* "dormancy" and phenotypic drug resistance: decreased pH, hypoxia, iron deprivation, and nutrient shift or depletion. We highlight knowledge gaps that should be filled to develop predictive *in vitro* assays for the discovery and development of shorter treatment regimens.

HOW DOES CASEUM FORM AND CONTRIBUTE TO DISEASE?

Two schools of thoughts promote partially overlapping concepts, both highlighting the prominent role of lipids and lipid-laden (foamy) macrophages in the generation of caseous necrosis. When cellular lipid homeostasis is perturbed by pathological conditions, such as sustained inflammation, lipid droplets may accumulate in the cytoplasm of macrophages (18). One theory proposes that postprimary tuberculosis begins as localized foci of lipid pneumonia in the alveolar space, where infection of alveolar macrophages triggers their differentiation into foamy macrophages. In early postprimary TB, cavities would develop by necrosis of tuberculous lipid pneumonia rather than

through erosion of caseating granulomas into bronchi (19–21). This paradigm largely emerged in the preantibiotic era, when TB-related deaths and subsequent autopsies were more frequent. Today's prevalent views favor the thesis that the primary site of caseation is the central core of a granuloma, where multiple coordinated events lead to the necrosis of epithelioid foamy macrophages (22, 23). Subsequently, an expanding necrotic granuloma may erode into a nearby airway and coalesce with its wall, forming a cavity, the prerequisite to disease transmission. Both types of pathologies were recognized as early as 1821 by Laennec (24). They were described as "exudative," referring to pneumonia, and "productive," referring to nodular tubercles or granulomas. As access to untreated clinical samples declined and with the rise of animal models that reproduce primary rather than postprimary TB, the concept of lipid pneumonia as an early source of caseation has been displaced by the caseating granuloma, although the two types of pathologies are not mutually exclusive.

The induction of foam cell formation is multifactorial and only partially understood. *In vitro*, infection of macrophages by *M. tuberculosis* causes intracellular lipid accumulation that exceeds the host cell's capacity to maintain lipid homeostasis (25). Stimulation of lipid-sensing nuclear receptors, Toll-like receptors, and other membrane-bound macrophage receptors by *M. tuberculosis* cell wall lipids, including oxygenated mycolic acids, is involved in foam cell biogenesis (23, 26, 27). Host lipids are sequestered in lipid droplets that form in the endoplasmic reticulum and accumulate within the cytosol, giving the cells their characteristic "foamy" appearance (22, 23, 25). Other triggers of foaminess, with potential *in vivo* relevance, have been demonstrated and characterized *in vitro*: hypoxia and exposure to very-low-density lipoproteins and to selected fatty acids (28–30). Because lipid droplets are intimately connected to immune modulation, critical macrophage immune functions such as autophagy are diminished, which could facilitate intracellular survival and persistence of *M. tuberculosis* in the host (18, 31).

Several experimental findings support the view that caseum is largely made of necrotized foamy macrophages. In clinical samples and animal models, foamy macrophages directly surround the caseous core of necrotic granulomas (10, 23, 25, 32), consistent with the idea that their necrotic death leads to the release of lipid droplets and cellular debris at the caseum interface. However, the mechanisms leading to foamy macrophage cell death, whether apoptotic or necrotic, are only partially understood. According to a long-held belief, in a cytotoxic delayed-type hypersensitivity reaction, activated T lymphocyte-mediated killing of infected foamy macrophages destroys local tissue, leading to expansion of the caseous center of the granuloma and release of extracellular bacilli (21, 33, 34). The paradigm that human T cell responses contribute to the lung tissue destruction underlying cavitary TB is consistent with the low frequency of cavitation among HIV-TB patients and the linear correlation between the number of circulating $CD4^+$ T cells and the frequency of cavitary TB (35). However, much remains to be elucidated on the mechanisms triggering foamy macrophage death at the cellular/necrotic interface of granulomas.

Investigation of the molecular composition of caseum, on the other hand, is rapidly progressing. Using a range of biochemical and molecular techniques, Kim et al. have shown that the protein, nucleic acid, and lipid composition of caseum bears numerous similarities with that of foamy macrophages. Genes involved in lipid sequestration and metabolism were highly expressed in human caseous granulomas, and the products of these genes were similarly overrepresented in cells surrounding the caseum. Furthermore, they determined that the most abundant lipid species in caseum are also dominant in *in vitro M. tuberculosis*-infected foamy macrophages that acquire lipids from low-density lipoproteins (LDLs) (22). These observations suggest that induction of foam cell formation by *M. tuberculosis* may represent a mechanism by which the pathogen drives the progression of the granuloma toward cavitation and transmission (36). They are also consistent with the view that lipid-laden foam cells contribute to TB disease pathology.

Neutrophils have been the center of renewed and rising interest in TB disease

progression and pathology (their damaging and protective roles are comprehensively and elegantly reviewed elsewhere) (37, 38). They are an important component of exudative lesions (39) and granulomatous lesions of both TB patients and animal models (10, 40). The extent of neutrophil infiltration in caseum is highly variable, even within different lesions of the same host. In caseous foci where neutrophils are found in high numbers, they are associated with high pathogen load (38). *In vitro* studies suggest that necrotic neutrophils may exert detrimental effects on the host response in active TB (41), an important finding given the relatively short life span of neutrophils and long residence time in caseum in the absence of an active drainage system. In sputum, bronchoalveolar lavage fluid, and pulmonary TB cavity contents, neutrophils are a dominant cell type, again implying that neutrophilic inflammation can be a manifestation of failed immunity to *M. tuberculosis* in humans (42). In short, *M. tuberculosis* appears to utilize exquisite strategies to evade neutrophil-mediated immunity and exploits neutrophilic inflammation to preferentially replicate at sites of tissue damage such as necrotic foci (43). In the C3HeB/FeJ mouse model, massive neutrophilic infiltration correlated with liquefactive necrosis (44), a concept that has gained momentum recently but remains to be demonstrated in clinical TB. Caseum liquefaction is an *in vivo* phenomenon, occasionally observed in selected animal models, and thus a challenging field of study. In 1955, Canetti discussed four possible mechanisms underlying caseum liquefaction, based on microscopy, biochemical, and histological analyses of human autopsy samples: (i) the release of proteolytic enzymes during a secondary non-TB infection, (ii) the reactivation of proteolytic enzymes from necrotized host cells, (iii) the influx of polymorphonuclear cells, and (iv) robust *M. tuberculosis* growth (45). Caseous foci appeared to disintegrate into viscid masses of varied consistencies, and intermediary stages between solid and liquid caseum were often observed (45).

In a more recent review of the liquefaction process, the authors speculate that lesions in the upper lobes of the lungs are more prone to liquefaction because higher oxygen tension favors increased bacterial growth, which is further enhanced by reduced immunological surveillance due to reduced blood flow in this part of the lungs (46). Overall, high neutrophil numbers, liquefaction, and increased multiplication of extracellular bacilli have been found in many studies to be intertwined (46); however, causality relationships between these features remain to be clearly established. Regardless of liquefaction processes, clinical data strongly suggest that cavitary TB disease is associated with higher bacterial burdens, disease transmission, and the requirement of longer therapy duration (1, 47–50).

M. TUBERCULOSIS IN CASEUM

Detection

The acid-fast (AF) stain, also known as Ziehl-Neelsen (ZN) stain, is the traditional microscopic detection method for the diagnosis of TB infection in patient sputum. Consistent with the concept that expectorated sputum drains liquefied cavity caseum, acid-fast stains of necrotic granulomas from C3HeB/FeJ mice, guinea pigs, rabbits, and humans reveal large extracellular subpopulations within the acellular matrix of the caseous loci (3, 4, 10, 32, 51–53). The conversion of *M. tuberculosis* from the AF-positive form during active replication to the AF-negative form during dormancy was reviewed recently by Vilcheze and Kremer (54). Called Koch's paradox, this phenomenon has been observed in both clinical specimens and animal models of TB infection. For instance, mycobacterial titers of lung homogenates of chronically infected mice are maintained during the later stages of infection, while AF detection of bacterial burden is significantly reduced (55). Additionally, tissue sections from patients with latent TB infections (LTBI) are positive for staining with pAbBCG, a polyclonal antibody, but remain AF negative. This is in contrast with tissue sections from patients with acute or reactivated TB, which are positive for both stains (55, 56). Although the precise cell wall components involved in AF staining remain incompletely described, mycolic acids and

other cell wall-associated (glyco)lipids are known to play an important role. Changes in the composition and spatial architecture of these lipids in the cell wall lead to the AF-negative phenotype (54). However, the recent discovery that cytokinin-induced expression of Rv0077c also results in the loss of acid-fastness in *M. tuberculosis* without accompanying alterations in the mycolic acid profile highlights that this phenomenon is driven by several distinct mechanisms (57). Rhodamine-auramine staining of mycobacteria, which is also cell wall composition dependent, is similarly lost during dormancy in AF-negative bacilli (55).

ZN staining of the caseous foci of closed necrotic granulomas and cavities revealed that the distribution of AF-positive *M. tuberculosis* bacilli is highly heterogeneous, with distinctly visible regions of high and low bacterial burdens (51). Given the nonreplicating status of caseum *M. tuberculosis*, the standard ZN staining technique may not be sufficiently sensitive to completely visualize this subpopulation. To overcome this issue, Blanc et al. developed a matrix-assisted laser desorption ionization mass spectrometry imaging (MALDI-MSI) technique capable of detecting and mapping the two-dimensional distribution of abundant *M. tuberculosis* cell wall lipids (51). They successfully imaged multiple phosphatidylinositol mannoside (PIM) species and their precursors in the caseous granulomas of infected rabbits and C3HeB/FeJ mice. The precise colocation of these lipid biomarkers with bacilli in thin tissue sections indicates that these cell wall lipids are not secreted and do not spread within lesions. This technique does not allow visualization of individual bacilli due to (i) limited sensitivity and (ii) limited spatial resolution (50 by 50 μm, or the size of a pixel in MALDI MS images), which approximately corresponds to clusters of 5 to 10 bacilli where bacterial burden is high (51). Alternatively, bacteria can be labeled with fluorescent *M. tuberculosis*-specific antibodies and detected by confocal microscopy imaging (55, 58). The SYBR gold stain is also capable of detecting replicating and nonreplicating *M. tuberculosis* by intercalating with DNA and RNA regardless of the pathogen's metabolic state (53, 59). These confocal microscopy techniques have the advantage of single-cell resolution but consume resources and time.

Bacterial Burden

Information regarding the specific bacterial burden of caseum is scarce because clinical and preclinical studies often provide bacterial counts for entire lung organs or whole dissected granulomas, at best, but not distinct lesion compartments such as the cellular rim versus caseous center. The overall burden of necrotic granulomas is often used as a surrogate to assess the burden of the caseous cores. Bacterial burden estimates date from the preantibiotic era, when autopsies of TB patients were accessible.

In humans, necrotic lesions are thought to persist for extended durations without complete healing while the central caseous compartment hardens and calcifies (45). It is believed that during this process, the majority of the *M. tuberculosis* burden in caseum dies over time while a small subpopulation survives in a state of limited metabolic activity. This was concluded through systematic enumeration of ZN-stained bacilli in thin sections of multiple clinical pulmonary lesions, which showed that the bacillary content of younger, nuclear debris-rich caseum is significantly higher than that of more advanced and mature caseum (45). The same study showed that (i) mature solid caseum with homogenous necrosis often yielded no or very few AF-positive bacilli and (ii) liquefied caseum can sometimes be the site of explosive *M. tuberculosis* multiplication. Multiple fields of view within the same human caseous nodule revealed zones of solid caseum with no visible bacilli and zones of liquefaction containing thousands (45). In 1965, Canetti determined that pulmonary TB cavities of patients harbor as much as 10^7 to 10^9 bacilli, in contrast to only 10^2 to 10^4 bacilli in closed necrotic lesions (60). Since the high oxygen content of airways favors *M. tuberculosis* growth, the development of cavitary disease marks the first burst of extracellular multiplication since the onset of infection (33). In our recent study, we noted that the *M. tuberculosis* burden of cavity caseum excised from rabbit lung ranges from 6×10^5

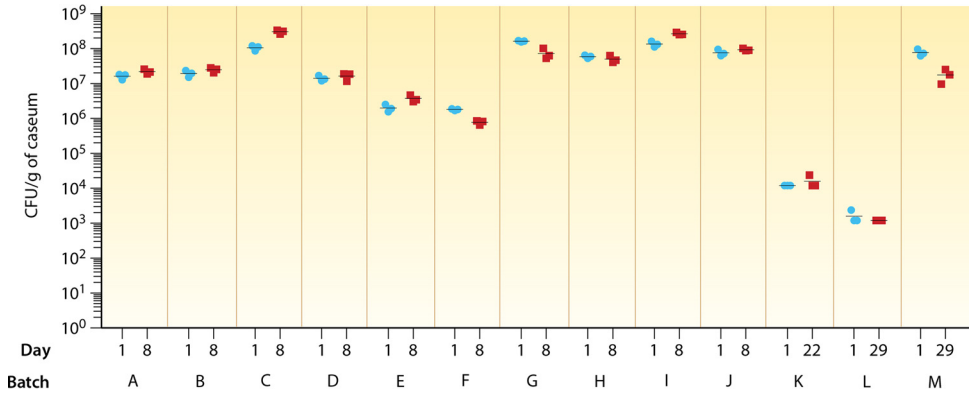

FIG 1 Bacterial burden and growth kinetics of *M. tuberculosis* in *ex vivo* rabbit caseum. Bacterial burdens on day 1 and day 8, 22, or 29 after excision of caseum from 13 rabbit cavities are shown. *M. tuberculosis* in caseum appears to be nonreplicating over the whole incubation period. Adapted from the work of Sarathy et al. (13).

to 3×10^8 CFU per gram of tissue (13). This range is dramatically higher than in seemingly uninvolved lung sections (0 to 1.0×10^3 CFU/g) and in cellular lesions (0 to 3.2×10^4 CFU/g) from chronically infected rabbits (10). Necrotic lesions from these rabbits harbor only up to 2.3×10^5 CFU/g, confirming that *M. tuberculosis* replication increases dramatically upon the reintroduction of oxygen when closed nodules transform into cavities.

Differentially culturable tubercle bacilli (DCTB) constitute a subpopulation of *M. tuberculosis* that escapes detection by standard culture methods (61). They do not grow when plated on solid media but can do so in liquid media that has been supplemented with *M. tuberculosis* culture filtrate or recombinant resuscitation-promoting factors (Rpfs) (62). Importantly, DCTB often fails to respond to antibiotic treatment in the way that readily detectable *M. tuberculosis* does (61). Sputum from TB patients harbors a variable but significant proportion of DCTB (62–64). Since it is widely accepted that sputum *M. tuberculosis* originates from pulmonary cavities, this raises the possibility that caseum may also harbor a significant DCTB subpopulation. The enumeration of *M. tuberculosis* burden in tissues is traditionally achieved by "plating" homogenates onto agar media, but this method would not account for DCTB. Indeed, lung tissue specimens from latently infected rabbits, for instance, appear sterile on agar media until animals receive an immunosuppressive agent, which facilitates *ex vivo* bacillary growth of what the authors refer to as "dormant *M. tuberculosis*" (58). Further studies using Rpf-supplemented liquid media are required to improve bacterial detection in seemingly sterile and low-burden caseum specimens.

Replication State

In the caseous core of necrotic granulomas, *M. tuberculosis* bacilli are thought to exist in a slow or nonreplicating state, mostly because the avascular and necrotic nature of this microenvironment generates hypoxic conditions which, in turn, induce nonreplicating persistence in mycobacteria (56, 65–67). In addition, the sustained release of necrotizing foamy macrophages in caseum is thought to increase oxygen- and nitrogen-reactive species, also known to induce nonreplicating persistence (68, 69). *In vitro* models designed to mimic these environmental stressors correspondingly shift replicating *M. tuberculosis* to the nonreplicating state (65, 70–72). However, direct evidence of nonreplicating *M. tuberculosis* in caseum was lacking until recently. Using caseum excised from the lung cavities of TB-infected rabbits, we provided first proof of this phenomenon, showing that the bacterial burden of caseum samples remained constant when the samples were incubated *ex vivo* for up to 28 days at 37°C (Fig. 1) (13).

To determine whether the constant CFU profile was the result of true nonreplication versus balanced growth and death, we measured bacterial chromosome equivalents

(CEQ), which reflect the cumulative burden of live and dead bacteria in the lesion, and CEQ/CFU ratios, indicative of the extent of bacterial killing over time (73). In all *ex vivo* caseum samples analyzed, both CEQ and CEQ/CFU ratios remained constant, indicating true nonreplication rather than a balance between growth and death. Interestingly, we have observed a wide range of CEQ/CFU ratios in rabbit caseum specimens, indicative of a large spectrum from robust immune-mediated killing to failed immunity. This observation agrees with previous studies that have noted heterogeneity in the extent of immune-mediated killing of *M. tuberculosis* in lesions from rabbits and cynomolgus macaques (10, 12).

Intracellular Lipophilic Inclusions

Intracellular lipophilic inclusions (ILIs) were first observed in *M. tuberculosis* by Burdon in 1946 (74). Since then, they have been visualized in multiple mycobacterial species using electron microscopy and a combination of confocal microscopy and auramine-O/Nile red dual staining (75). Both techniques have clearly revealed ILIs in *M. tuberculosis* from clinical sputum samples (76–78). The ILI-positive subpopulation in sputum samples accounts for 3% to 86% of the total quantity of *M. tuberculosis* organisms detected (77). Using auramine-O/Nile red dual staining, we recently showed that a large proportion of *M. tuberculosis* bacilli in rabbit caseum contain ILIs, the first such evidence in any caseum specimens (13). Most ILI-positive bacilli did not stain with auramine, suggesting a loss of acid-fastness of caseum *M. tuberculosis* as described by others (79–81).

The major lipid species found in lipid extracts from ILI-rich *M. tuberculosis* include triacylglycerols (TAGs), fatty acids (FAs), polar lipids, and wax esters (WEs) (79, 80, 82). TAGs, which are nonpolar and water insoluble, are a better long-term form of stored carbon-based energy than carbohydrates and proteins because they are less sensitive to oxidation and have higher calorific value (83). TAG storage and utilization are widespread among eukaryotic organisms, such as yeasts, fungi, plants, and animals, but uncommon among bacteria with the exception of the *Actinomycetes* group, which includes mycobacteria (83). The exhaustive lipid composition of ILIs from caseum *M. tuberculosis* has yet to be determined. However, we know that ILI lipid reserves are a direct reflection of the FA building blocks available in its immediate external milieu. It has been shown that FA compositions of host macrophage TAGs and intracellular *M. tuberculosis* TAGs are nearly identical, suggesting that the pathogen derives FA from host TAGs for incorporation into its private ILI stores. *M. tuberculosis* in oleic acid-induced foamy macrophages accumulate TAGs consisting of $C_{16:0}$, $C_{18:0}$, and $C_{18:1}$ FAs predominantly and $C_{24:0}$, $C_{26:0}$, and $C_{28:0}$ to a much lesser extent (80). In axenic cultures, *M. tuberculosis* under hypoxia accumulates TAGs and WEs with $C_{16:0}$ and $C_{18:0}$ as the major FA constituents (79). Supplemented oleic acid is specifically incorporated into $C_{26:0}$-containing TAGs, whereas acetate and palmitate are incorporated into $C_{16:0}$- to $C_{26:0}$-containing TAGs and $C_{14:0}$- to $C_{28:0}$-containing TAGs, respectively (84).

The presence of ILIs in *M. tuberculosis in vivo* is significant because there is overwhelming evidence of its strong association with the state of dormancy and phenotypic resistance to rifampin and isoniazid (77, 79–82). The removal of lipid supplementation and reversal of ILI accumulation leads to the resumption of mycobacterial cell division (85). In sputum samples from drug-naive patients, a higher frequency of ILI-positive *M. tuberculosis* correlates with longer time to positivity, consistent with the notion that they are slowly replicating or nonreplicating bacteria (77). *In vitro* assays using single and multiple stress nonreplication models induce accumulation of ILIs in *M. tuberculosis*, with corresponding drastic increases in triacylglycerol synthase (*tgs1*) gene expression (77, 79). Collectively, the evidence suggests that the *M. tuberculosis tgs1* gene product is responsible for the re-esterification of host lipid-derived FAs into TAGs for intrabacterial storage in response to environmental stresses. The Δ*tgs1* deletion mutant is hence severely compromised in its ability to accumulate TAGs under various stress conditions, fails to develop tolerance to antibiotics, and is more likely to be AF positive

(79, 80, 86). Fifteen putative triglyceride synthases (encoded by *tgs* genes), also known as diacylglycerol transferases, were identified in *M. tuberculosis*, and all showed TGS activity when expressed in *Escherichia coli*. Of these genes, *tgs1* (*rv3130c*) is the most active and the most induced in nonreplicating persistent bacilli (84). *tgs1* lies in close proximity to the dormancy transcription factor gene *dosR*, and disruption of the latter completely prevents the induction of *tgs1* under hypoxia (87). Members of the triacylglycerol synthase family are differentially regulated at the transcription level, and some members are exclusively present in pathogenic mycobacteria (88).

Daniel et al. identified PPE15, a perilipin-like protein in *M. tuberculosis* that regulates lipid droplet homeostasis. The PPE15 knockout mutant is compromised in its ability to accumulate TAG and develop tolerance to rifampin (82). Furthermore, Rv2744c, an ortholog of phage shock protein A (PspA), localizes to the surface of ILIs, where it oligomerizes, and regulates ILI number and size and *M. tuberculosis* survival in the nonreplicating persistent state (89). Utilization of energy stored as TAGs requires hydrolytic activity to release FAs for β-oxidation. Of the 24 putative lipases identified in *M. tuberculosis*, the product of *rv3097c* (LipY) has the highest hydrolytic activity and is most induced under stress. Correspondingly, the *lipY* deletion mutant is unable to utilize stored TAGs as efficiently as wild-type *M. tuberculosis* (90) and resuscitate from dormancy (81).

Pacl et al. presented an alternative hypothesis in which hypoxia and lipid metabolism saturate the electron transport chain and this reductive stress is balanced in part by lipid synthesis in a DosR/S/T-dependent manner (91). Interestingly, strains belonging to the Beijing lineage of *M. tuberculosis*, which is associated with increased pathogenicity and a higher propensity for developing drug resistance, accumulate TAGs more readily than other strains (92). This has been attributed to the constitutive overexpression of genes of the dormancy regulon, including *tgs1* (*rv3130*). The Beijing strains may be "preadapted" to stressful environmental conditions, such as hypoxia in caseous granulomas, and their abundant energy stores could confer an advantage over other lineages during latency and transmission (92). *Mycobacterium avium*, *Mycobacterium marinum*, and *Mycobacterium canetti*, to name a few other mycobacterial species, have been shown to develop lipid inclusions as well (85, 93, 94). However, ILI formation in intracellular *M. marinum* is not accompanied by growth arrest or decreased metabolic activity (93).

Drug Susceptibility

In recent studies, our group measured the susceptibility of *M. tuberculosis* present in rabbit cavity caseum to major first- and second-line anti-TB drugs (11, 13). This *ex vivo* assay involves exposing *M. tuberculosis* present in excised caseum to a range of concentrations of a drug or drug candidate over 7 days and determining the minimum concentration required to kill 90% of the bacteria present in the sample ($casMBC_{90}$) and the concentration required to fully sterilize caseum when applicable. Results clearly indicate that *M. tuberculosis* in caseum is profoundly tolerant to TB drugs. Depending on the drug, there was a 3- to 400-fold increase in MBC_{90} compared to that for replicating *M. tuberculosis* cultures (Table 1). Only the rifamycins and fluoroquinolones were effective at killing this *M. tuberculosis* subpopulation ($casMBC_{90} < 10\ \mu M$). Interestingly, rifamycins are the only drug class capable of fully sterilizing caseum specimens, albeit at relatively high concentrations (50 to 100 μM). This suggests that caseum *M. tuberculosis* is vulnerable to RpoB inhibition, at least via the specific mechanism of action of rifamycins. Bedaquiline, linezolid, and pyrazinamide performed modestly in the assay ($casMBC_{90}$ of 32 to 512 μM), whereas isoniazid, clofazimine, and kanamycin showed marginal to no activity (13). We have expanded the panel of TB drugs tested in this bactericidal assay, and all results support the notion of extreme drug tolerance of caseum *M. tuberculosis*. Results from the casMBC assay were compared with results from the nutrient starvation (Loebel) and oxygen deprivation (Wayne) models, both of which are frequently used to test drug susceptibility of nonreplicating *M. tuberculosis* (65, 95) (Table 1). The general trend across all three assays is a striking loss of

TABLE 1 Bactericidal activities of TB drugs against *M. tuberculosis* in *ex vivo* caseum and *in vitro* under replicating and nonreplicating conditions[a]

Antibiotic	Caseum MBC_{90} (μM)	MBC_{90} (μM)[b]	WCC_{90} (μM)[b]	LCC_{90} (μM)[b]
Isoniazid	>128	0.31–0.63	>100	>100
Pyrazinamide	512	>80	>100	>100
Rifampin	8	0.078	1	10
Rifapentine	2	0.078	0.5	10
Rifabutin	2	0.039	0.5	10
Rifalazil	2	0.036[c]		
Moxifloxacin	2	0.31–0.63	10	>100
Levofloxacin	8	1.25–2.5	50	>100
Gatifloxacin	2	0.63	50	>100
Linezolid	128	10	>100	>100
Radezolid	2			
Pretomanid	32	0.63	20	
Kanamycin	>128	5.0	20	>100
Clofazimine	>128	40	50	>100
Bedaquiline	32	10	>20	>20

[a]Adapted from the work of Sarathy et al. (13). MBC_{90}, minimum concentration required to kill 90% of the bacterial population; WCC, Wayne (hypoxic culture) bactericidal concentration; LCC, Loebel (nutrient starved culture) bactericidal concentration.
[b]Most MBC and all WCC and LCC data were obtained from Lakshminarayana et al. (119).
[c]MBC_{90} data for rifalazil were obtained from Mor et al. (153).

bactericidal activity. Overall, drug potencies were more similar in Wayne versus casMBC than in Loebel versus casMBC assays. Most notable differences between the Wayne and casMBC assays were found with the fluoroquinolones, markedly more potent in caseum, and kanamycin as a representative of aminoglycosides, much less potent in caseum (13). These two antibiotic classes are currently the mainstay of second-line therapy against multidrug-resistant TB. Thus, the TB community still lacks a potency assay that is compatible with medium- to high-throughput requirements and reproduces the drug tolerance of caseum *M. tuberculosis*.

ENVIRONMENTAL STRESS FACTORS

Given the persistent nature of caseum *M. tuberculosis*, understanding this subpopulation is key to shortening treatment duration and improving cure rates. In this section, we examine the environmental stress factors that are often credited for triggering the shift of caseum *M. tuberculosis* to the nongrowing state.

Acidic pH

The acidity of caseum is important because *M. tuberculosis* growth *in vitro*—whether in nutrient-rich or minimal medium—slows at acidic pH (<6.5) and is completely halted at pH 5.0 (71, 96, 97). However, the organism remains viable since it can resist external pH as low as 4.5 and maintain neutral cytosolic pH (98, 99). The notion that the caseous core of necrotic granulomas forms an acidic microenvironment has been promoted since the 1950s, most likely as an explanation for the remarkable treatment-shortening capacity of pyrazinamide, which is more potent *in vitro* at acidic pH (100, 101). As summarized in Table 2, the pH of caseous foci of mice, guinea pigs, and rabbits is, on average, close to neutral. A study from 1954 with TB-infected rabbits showed that caseum pH increased from 6.4 to 7.4 as lesions matured and liquefied (102). In contrast, Kempker et al. measured the pH of caseum in the lesions of 10 pyrazinamide-treated TB patients using indicator strips and found a median pH of 5.5, with a range of 5 to 7.2, and only 2 readings exceeding pH 7.0. Both tissue samples with neutral caseum presented severe necrosis and an abundance of AF-staining bacilli (103). In older studies of human caseum specimens, more neutral conditions were observed (104, 105). These observations collectively indicate that acidity is not the primary environmental pressure contributing to caseum *M. tuberculosis*'s nonreplication and the drug-tolerant phenotype. It seems more likely that cytosolic pH homeostasis in *M. tuberculosis* evolved to combat phagosome acidification as opposed to acidification of caseum.

TABLE 2 Measurement of pH of caseum in various species using different techniques

Species	Nature of specimen	Measurement technique	pH range	Reference
C3HeB/FeJ mouse	*In situ*	16-gauge needle tip micro-pH electrode	7.2–7.5 (7.4[a])	154
	Homogenate	pH indicator strips	7.4–7.6	9
Guinea pig	*In situ*	16-gauge needle tip micro-pH electrode	7.0–7.5 (7.2[a])	150
Rabbit	3-fold diluted in water	pH indicator strips	7.0–7.5	13
	Undiluted smear	pH indicator strips	6.1–8.0 (6.7[b])	10
	Homogenate in sucrose solution	Glass electrode	6.4–7.4	102
Human	*In situ*	pH indicator strips	5–7.1 (5.5[b])	103
	Homogenate	Glass electrode	7.3–8	104
	Aspirates[c]	Glass electrode	7.2–7.5	105

[a]Mean.
[b]Median.
[c]Nonpulmonary TB.

The phagosomal compartment in which mycobacteria resides during intracellular infections has a pH range of 4.5 to 6.5 depending on the activation state of the macrophage (106–108).

Hypoxia

Low oxygen tension is a widely accepted feature of necrotic granulomas given the lack of vascularization in the caseous core. Tsai et al. confirmed the absence of endothelial cells in the necrotic region of human TB lung granulomas by observing a lack of immunoreactivity with anti-CD31 antibodies (109). The fibrotic cuff of more mature granulomas theoretically further reduces its ability to "breathe." Table 3 summarizes published observations of hypoxia in TB granulomas from various animal infection models and the detection techniques used. The oncology probe pimonidazole hydrochloride (PIMO) has been useful for the visualization of hypoxic regions in mammalian and human tumors (110). Also known as Hypoxyprobe, PIMO is bioreductively activated by mammalian nitroreductases at low oxygen concentrations and binds to thiol groups on cellular proteins, forming adducts that can be detected with specific antibodies. Prolonged oxygen tensions of $\leq$10 mm Hg are required for thiol adduct formation. Via et al. infused TB-infected guinea pigs, rabbits, and cynomolgus ma-

TABLE 3 Detection of hypoxic granulomas in various species using different techniques[a]

Species	Caseous necrosis	Measurement technique	pO_2	Reference
BALB/c mouse	Absent	Immunodetection of PIMO	Not hypoxic	8
		[^{64}Cu]ATSM PET imaging	Not hypoxic	8
C57BL/6 mouse	Absent	Immunodetection of EF5	Not hypoxic	109
		Immunodetection of PIMO	Not hypoxic	115
		Catheter microelectrode	Not hypoxic	115
C3HeB/FeJ mouse	Present	Immunodetection of PIMO	$<$10 mm Hg	8
		Immunodetection of PIMO	$<$10 mm Hg	7
		[^{64}Cu]ATSM PET imaging	$<$3.8 mm Hg	8
Guinea pig	Present	Immunodetection of PIMO	$<$10 mm Hg	111
		Immunodetection of PIMO	$<$10 mm Hg	3
Rabbit	Present	Immunodetection of PIMO	$<$10 mm Hg	111
		Fiber optic oxygen sensor	1.6 mm Hg	111
Cynomolgus macaque	Present	Immunodetection of PIMO	$<$10 mm Hg	111
		Immunodetection of PIMO	$<$10 mm Hg	122
Human	Present	[^{18}F]FMISO PET-CT imaging	$<$10 mm Hg	113

[a][^{64}Cu] ATSM PET, ^{64}Cu-diacetyl-bis (*N*^{4}-methylthiosemicarbazone) positron emission tomography; EF5, 2-(2-nitro-1H-imidazol-1-yl)-*N*-(2,2,3,3,3-[18F]pentafluoropropyl)-acetamide; PIMO, pimonidazole hydrochloride; [^{18}F]FMISO, [^{18}F]fluoromisonidazole.

caques with PIMO prior to necropsy and showed distinct regions of adduct formation in the caseous core of pulmonary necrotic granulomas in all three species (111). Lenaerts et al. similarly used PIMO to visualize hypoxic regions of necrotic granulomas in the guinea pig model of TB infection and found that persistent *M. tuberculosis* in the necrotic pulmonary lesions of antibiotic-treated guinea pigs are primarily located within the hypoxic caseous foci. In this animal model, hypoxic regions of caseous granulomas are established as early as 30 days after infection, meaning that oxygen deprivation is not just a feature of persistent or latent infections (3). In both studies, PIMO staining appears as a characteristic ring encircling the caseous center because deep necrotic tissue is devoid of viable cells that reduce PIMO and facilitate adduct formation. Therefore, an assumption is made regarding anaerobicity in the deepest regions of the caseous core (3, 111). The former study also provided further evidence of hypoxia by using a fiber optic oxygen sensor inserted directly into the granulomas of infected rabbits. The mean oxygen partial pressure of TB granulomas with caseous centers was 1.6 mm Hg, 37-fold lower than that of seemingly normal sections of lung. It is worth mentioning that cavities have the highest oxygenation levels of all TB lesion types, as their surface is in contact with the airway and has an oxygen tension similar to that of the communicating bronchi (112). Therefore, *M. tuberculosis* residing in cavity caseum likely encounters only limited hypoxic stress that could be present in the deeper layers of cavity caseum toward the cellular and fibrotic wall.

Positron emission tomography (PET)-computed tomography (CT) scans of TB patients dosed with the hypoxia-specific tracer [^{18}F]fluoromisonidazole ([^{18}F]FMISO) showed distinctive accumulation of [^{18}F]FMISO in lesions and the regions surrounding cavities. Heterogeneous degrees of hypoxia were observed within and between lesions, consistent with the concept of multiple diverse TB microenvironments within individual patients (113). However, PET-CT does not allow for the colocalization of FMISO "hot spots" with caseum. Neither BALB/c nor C57BL/6 mice develop necrotic lesions with caseous centers upon TB infection (32, 114). Using the hypoxic tracer copper(II)-diacetyl-bis(N^4-methyl-thiosemicarbazone) ([^{64}Cu]ATSM), hypoxic necrotic granulomas were detected in TB-infected C3HeB/FeJ mice but not in BALB/c mice. These results were confirmed by PIMO immunostaining in the same study (8). Similarly, granulomas from C57BL/6 mice are not stained by PIMO or EF5, another hypoxia-sensitive compound which forms thiol adducts that can be immunodetected (109, 115).

As mentioned previously, bacterial burden is significantly higher in pulmonary cavities than in closed necrotic lesions (60), due to the reintroduction of oxygen and the subsequent resumption of bacterial replication. The implications of hypoxic condition in caseum are significant because an *in vitro* model that gradually depletes oxygen and then maintains low oxygen tension (Wayne model) triggers an adaptive dormancy response in *M. tuberculosis* (65, 116). In this model, *M. tuberculosis* arrests replication, decreases intracellular ATP levels (117), represses an array of cellular functions, including protein and DNA synthesis (118), and develops phenotypic resistance to most TB-active antibiotics (119, 120). At the molecular level, the dormancy response to hypoxia is mediated by the transcription factor Rv3133c, or DosR (for dormancy survival regulator) (87, 118, 121). Consequently, greater PIMO staining of granulomas from macaques with LTBI versus those from individuals with the active disease corresponded with higher induction of the DosR regulon in the former. In the same study, the strongest induction of the DosR regulon was observed in the most hypoxic tissue regions (i.e., caseum from LTBI granulomas) (122).

These findings highlight the value of animal models that reproduce caseous necrosis, fibrosis, and/or cavitation. These include the C3HeB/FeJ mouse, guinea pig, minipig, rabbit, and nonhuman primate models (32, 123, 124). Murine models in which the bulk of the bacterial population resides in immune cells—such as BALB/c and C57Bl6—and do not develop hypoxic necrotic lesions may be useful for the evaluation of drug efficacy against intracellular bacteria but do not reveal the complexities of a persistent extracellular subpopulation (114).

Iron Starvation

Iron is essential for life of most organisms, including mycobacteria. *M. tuberculosis* uses an array of metal detoxification and acquisition systems to combat phagosome-centric host responses to infection, including iron and manganese deprivation and copper and zinc overload (125). The host's propensity to sequester iron for itself makes free iron a scarce commodity in the phagolysosomes of infected macrophages. *M. tuberculosis* overcomes iron deprivation via mechanisms that include siderophore-based ferric ion chelators, ABC-type heme transporters, and ferritin-based iron storage (126). Iron-starved growth-arrested *M. tuberculosis* is tolerant to several antibiotics (127). Whereas direct observation of depleted iron levels in caseum has not been made, iron limitation in human lesions is implied because of the following: (i) *M. tuberculosis* genes involved in iron homeostasis are required for virulence (128–130); (ii) "African iron overload," a condition associated with high dietary iron intake and specific genetic defects, is significantly associated with developing pulmonary TB and TB-related mortality (131, 132); and (iii) LTBI patients can experience reactivation of disease upon receiving iron supplementation as treatment for anemia, since iron loading enhances the growth of intracellular *M. tuberculosis* (133, 134).

The necrotic center of a caseous granuloma is enriched in host-derived transferrin, haptoglobin, hemopexin, lactoferrin, and lipocalin, all of which collectively sequester free Fe^{3+}, hemoglobin, heme, and siderophores (127, 135). Assuming that the relative abundance of iron-sequestering proteins is inversely proportional to iron bioavailability, Kurthkoti et al. concluded that caseum constitutes an iron-depleted environment and demonstrated using an *in vitro* iron starvation model that *M. tuberculosis* is capable of persisting in a nonreplicating state under these conditions (127). However, whether these proteins continue to actively sequester iron within dead cell debris as they do in nonnecrotic lesion areas is an open question. Interestingly, *M. tuberculosis* in an adipocyte model meant to mimic the lipid-rich environment of caseating granulomas downregulates the iron-responsive regulator IdeR, among other gene expression changes that suggest iron abundance (136). Finally, gene expression profiling in sputum *M. tuberculosis* did not reveal the induction of iron-scavenging genes, suggesting adequate iron supply in the cavities from which these bacilli originate (77). Collectively, these findings provide mostly indirect and at times conflicting information on the availability of iron in caseum. Direct quantitation of free iron in the caseous foci of TB granulomas is required to assess whether *M. tuberculosis* is iron starved in this environment.

Nutrient Deprivation or a Shift in Carbon Sources

Nutrient limitation or deprivation is thought to stimulate the nonreplicating persistent state in caseum *M. tuberculosis*. In 1933, Loebel et al. developed an *in vitro* culture model that maintains nonreplicating *M. tuberculosis* with a low metabolic rate in a nutrient-deprived oxygen-rich medium (Loebel model) (70), characterized by lowered intracellular ATP levels (137), decreased energy metabolism, lipid biosynthesis, and cell division, among other changes in the transcriptome (138). These changes are accompanied by decreased drug penetration and intracellular accumulation (139) and drastic losses in susceptibility to multiple anti-TB drugs (119, 137–139). However, the relevance of the Loebel culture medium—phosphate-buffered saline with Tween—to recapitulate nutrient conditions found in lesions is debatable.

Total lipid extraction from the caseous foci of human pulmonary caseous TB granulomas followed by thin-layer chromatography (TLC) and mass spectrometric analyses revealed marked accumulation of cholesterol, cholesterol esters (CEs), triacylglycerols (TAGs), and lactosylceramides (LacCer) compared to the levels in uninvolved normal lung tissue (22). Guerrini et al. subsequently conducted comprehensive liquid chromatography coupled to mass spectrometry (LC/MS) analyses of lipids from human, marmoset, and rabbit caseum specimens that were dissected by a laser capture microdissection (LCM) platform and found TAGs and CEs to be the predominant lipid classes. The TAG profiles from all three species were highly conserved, with three highly

abundant clusters: TAGs containing FA chains of (i) 50 carbons and 0 to 3 double bonds, (ii) 52 carbons and 0 to 4 double bonds, and (iii) 54 carbons and 1 to 5 double bonds. The CE profiles, on the other hand, were more variable within and between species (25). These findings suggest that rather than nutrient deprivation, *M. tuberculosis* is faced with a lipid-rich diet in caseum.

Indeed, the *M. tuberculosis* genome is loaded with about 250 genes encoding enzymes involved in FA metabolism, an impressive proportion of which are dedicated to FA degradation and oxidation, strongly suggesting that *M. tuberculosis* is committed to using host lipids *in vivo* (140). Electron microscopy images of infected foamy macrophages revealed the tight apposition of *M. tuberculosis*-containing phagosomes to macrophage lipid bodies followed by the appearance of ILIs, implying the internalization of lipid bodies into the phagosomes, where *M. tuberculosis* utilizes host-derived lipids (23, 141). Given the similarities in the lipid profiles of caseum and its surrounding ring of infected foamy macrophages (22, 25), it is likely that *M. tuberculosis* is similarly adapted to the utilization of caseous lipids as a nutrient source. The observation of lipid accumulation in caseum *M. tuberculosis* supports this hypothesis (13). The upregulation of isocitrate lyase (*icl1*), a member of the glyoxylate cycle, in ILI-rich *M. tuberculosis* also suggests a shift to utilizing FAs as a source of energy (77). Icl1 plays a second role in *M. tuberculosis* as a methylisocitrate lyase (MCL) in the methylcitrate cycle which degrades propionate, further enabling cholesterol utilization by *M. tuberculosis* (142). Other studies have also shown that *M. tuberculosis* is well adapted to metabolizing and utilizing cholesterol and FAs during the chronic phase of infection (143–147), both of which are abundant in caseous foci (22). Since *M. tuberculosis* bacilli found in caseum largely come from necrotized foamy macrophages where *M. tuberculosis* has already adapted to a lipid-rich environment and energy is stored in the form of ILIs, it is possible that little to no further metabolic adaptation is required when the bacteria transit from an intracellular lifestyle in lipid-laden macrophages to an extracellular existence in necrotic caseum.

CONCLUSION

In 1955, Canetti regarded caseation as the most important event of tuberculosis infection. *M. tuberculosis* manipulates the host's metabolism by inducing lipid accumulation in foamy macrophages (22), which subsequently necrotize and release their stored lipids, forming a CE- and TAG-rich reservoir in caseum, where the pathogen feeds and persists. *M. tuberculosis* is believed to remain dormant in caseous lesions for extended periods before reactivation and cavitation occur. The cavity surface is known as a microenvironment of failed immunity due to the selective absence of $CD4^+$ and $CD8^+$ T cells at the luminal surface (in contact with airways), preventing direct T cell-macrophage interactions at this site and allowing luminal phagocytes to remain permissive for bacillary growth (148). This provides the pathogen with a safe haven for robust replication and an outlet for transmission (149). Although plating on standard growth media has shown that the bacterial burden of caseous granulomas reaches high numbers in various animal models, we may still underestimate total counts and miss differentially culturable bacteria. New tools capable of detecting all viable *M. tuberculosis* in caseum are being developed to provide better information on the efficacy of antibiotic treatment and predict relapse.

Here we have revisited widely accepted concepts about loss of acid-fastness and the stress factors thought to trigger *M. tuberculosis*'s shift to the nongrowing state in caseum, leading to phenotypic drug resistance. (i) pH measurements in multiple animal models and in patients indicate that acidic conditions may be only transient (10, 13, 102, 150) and that caseum pH in mature lesions varies across lesions even within the same organism but remains near neutral overall. Additional pH measurements of resected human cavities using modern readouts are required to confirm caseum pH and pH variability across lesions and design *in vitro* potency assays that recapitulate *in vivo* conditions. (ii) Proof of hypoxia by immunostaining techniques and the lack of blood supply in caseum collectively point to oxygen deprivation as one major envi-

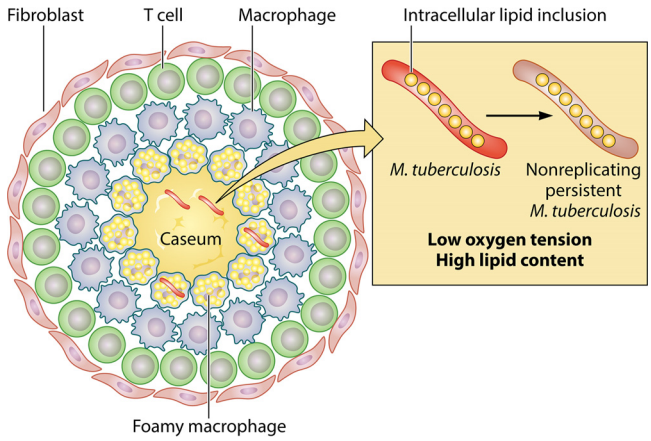

FIG 2 The caseous compartments of necrotic granulomas contain extracellular *M. tuberculosis*. This subpopulation adapts to local stresses such as low oxygen tension and high lipid content, resulting in the accumulation of intrabacterial lipid inclusions, a shift to a state of nonreplication, and phenotypic drug resistance. Created with BioRender.

ronmental pressure driving nonreplicating persistence in TB infections (151) (Fig. 2). While marked hypoxia is found in the caseum of closed granulomas, normoxic conditions are found at the cavity surface (112). It is likely that a gradient of oxygen tension exists from the surface of the cavity lumen—in direct contact with the airway—toward the deeper layers of caseum that border the cavity wall. Again, visualizing and quantifying such a gradient are critical to develop predictive *in vitro* potency assays. (iii) Deprivation of free iron and other trace elements in caseous foci is often implied by extension from the well-characterized iron sequestration in host cells. However, the equilibrium between bound and free iron in two oxidation states is a dynamic process that is likely not conserved in dead caseum and remains to be quantified. (iv) The abundance of lipid-based carbon sources in caseum and *M. tuberculosis*'s inclination for lipid catabolism (146, 147, 152) call into question the hypothesis that nutrient deprivation plays a significant role in the development of nonreplicating persistence.

Physiology and omics studies all point to a link between metabolic adaptations of *M. tuberculosis* to lipid-rich environments, ILI accumulation, and nonreplicating persistence (Fig. 2). Novel therapeutics that disrupt TAG hydrolysis, resynthesis, and storage in ILIs are likely to interfere with *M. tuberculosis*'s ability to survive in a lipid-rich microenvironment, inhibit the shift to nonreplication, increase susceptibility to antibiotics, and shorten treatment duration. Not surprisingly since caseum is largely made of necrotizing foamy macrophages, the microenvironmental conditions found in caseum are reminiscent of those present in infected macrophages and their phagolysosomes, suggesting that when released into caseum, *M. tuberculosis* is largely preadapted to the set of stressors it encounters (Fig. 2). The characteristics of caseum *M. tuberculosis* discussed in this review stem from observations of the pathogen at the population level but do not highlight heterogeneity in composition and physiological state of the caseous microenvironment and its residents, respectively, within each granuloma. This adds layers of complexity to understanding disease biology and treatment of this bacterial subpopulation. But advancements in the development of molecular probes and microscopy platforms should soon enable single-cell resolution while maintaining granuloma architecture and shed light on these issues. The major challenge for developing predictive and high-throughput assays that model the profound drug tolerance of caseum *M. tuberculosis* consists of reproducing the right balance of oxygen tension, pH, lipid abundance, and lipid species, using the *ex vivo* caseum bactericidal assay as a benchmark.

ACKNOWLEDGMENTS

This literature review was compiled with funding from grants U19-AI111143 from NIH-NIAID and OPP1174780 from the Bill and Melinda Gates Foundation.

REFERENCES

1. Palaci M, Dietze R, Hadad DJ, Ribeiro FK, Peres RL, Vinhas SA, Maciel EL, do Valle Dettoni V, Horter L, Boom WH, Johnson JL, Eisenach KD. 2007. Cavitary disease and quantitative sputum bacillary load in cases of pulmonary tuberculosis. J Clin Microbiol 45:4064–4066. https://doi.org/10.1128/JCM.01780-07.
2. World Health Organization. 2017. Treatment of tuberculosis. Guidelines for treatment of drug-susceptible tuberculosis and patient care. World Health Organization, Geneva, Switzerland.
3. Lenaerts AJ, Hoff D, Aly S, Ehlers S, Andries K, Cantarero L, Orme IM, Basaraba RJ. 2007. Location of persisting mycobacteria in a guinea pig model of tuberculosis revealed by r207910. Antimicrob Agents Chemother 51:3338–3345. https://doi.org/10.1128/AAC.00276-07.
4. Hoff DR, Ryan GJ, Driver ER, Ssemakulu CC, De Groote MA, Basaraba RJ, Lenaerts AJ. 2011. Location of intra- and extracellular M. tuberculosis populations in lungs of mice and guinea pigs during disease progression and after drug treatment. PLoS One 6:e17550. https://doi.org/10.1371/journal.pone.0017550.
5. Via LE, England K, Weiner DM, Schimel D, Zimmerman MD, Dayao E, Chen RY, Dodd LE, Richardson M, Robbins KK, Cai Y, Hammoud D, Herscovitch P, Dartois V, Flynn JL, Barry CE, III. 2015. A sterilizing tuberculosis treatment regimen is associated with faster clearance of bacteria in cavitary lesions in marmosets. Antimicrob Agents Chemother 59:4181–4189. https://doi.org/10.1128/AAC.00115-15.
6. Salkin D, Wayne LG. 1956. The bacteriology of resected tuberculous pulmonary lesions. I. The effect of interval between reversal of infectiousness and subsequent surgery. Am Rev Tuberc 74:376–387.
7. Driver ER, Ryan GJ, Hoff DR, Irwin SM, Basaraba RJ, Kramnik I, Lenaerts AJ. 2012. Evaluation of a mouse model of necrotic granuloma formation using C3HeB/FeJ mice for testing of drugs against Mycobacterium tuberculosis. Antimicrob Agents Chemother 56:3181–3195. https://doi.org/10.1128/AAC.00217-12.
8. Harper J, Skerry C, Davis SL, Tasneen R, Weir M, Kramnik I, Bishai WR, Pomper MG, Nuermberger EL, Jain SK. 2012. Mouse model of necrotic tuberculosis granulomas develops hypoxic lesions. J Infect Dis 205:595–602. https://doi.org/10.1093/infdis/jir786.
9. Irwin SM, Prideaux B, Lyon ER, Zimmerman MD, Brooks EJ, Schrupp CA, Chen C, Reichlen MJ, Asay BC, Voskuil MI, Nuermberger EL, Andries K, Lyons MA, Dartois V, Lenaerts AJ. 2016. Bedaquiline and pyrazinamide treatment responses are affected by pulmonary lesion heterogeneity in Mycobacterium tuberculosis infected C3HeB/FeJ mice. ACS Infect Dis 2:251–267. https://doi.org/10.1021/acsinfecdis.5b00127.
10. Blanc L, Sarathy JP, Alvarez Cabrera N, O'Brien P, Dias-Freedman I, Mina M, Sacchettini J, Savic RM, Gengenbacher M, Podell BK, Prideaux B, Ioerger T, Dick T, Dartois V. 2018. Impact of immunopathology on the antituberculous activity of pyrazinamide. J Exp Med 215:1975–1986. https://doi.org/10.1084/jem.20180518.
11. Sarathy J, Blanc L, Alvarez-Cabrera N, O'Brien P, Dias-Freedman I, Mina M, Zimmerman M, Kaya F, Liang HH, Prideaux B, Dietzold J, Salgame P, Savic R, Linderman J, Kirschner D, Pienaar E, Dartois V. 2019. Fluoroquinolone efficacy against tuberculosis is driven by penetration into lesions and activity against resident bacterial populations. Antimicrob Agents Chemother 63:e02516-18. https://doi.org/10.1128/AAC.02516-18.
12. Lin PL, Ford CB, Coleman MT, Myers AJ, Gawande R, Ioerger T, Sacchettini J, Fortune SM, Flynn JL. 2014. Sterilization of granulomas is common in active and latent tuberculosis despite within-host variability in bacterial killing. Nat Med 20:75–79. https://doi.org/10.1038/nm.3412.
13. Sarathy JP, Via LE, Weiner D, Blanc L, Boshoff H, Eugenin EA, Barry CE, III, Dartois VA. 2018. Extreme drug tolerance of Mycobacterium tuberculosis in caseum. Antimicrob Agents Chemother 62:e02266-17. https://doi.org/10.1128/AAC.02266-17.
14. Rifat D, Prideaux B, Savic RM, Urbanowski ME, Parsons TL, Luna B, Marzinke MA, Ordonez AA, DeMarco VP, Jain SK, Dartois V, Bishai WR, Dooley KE. 2018. Pharmacokinetics of rifapentine and rifampin in a rabbit model of tuberculosis and correlation with clinical trial data. Sci Transl Med 10:eaai7786. https://doi.org/10.1126/scitranslmed.aai7786.
15. Prideaux B, Via LE, Zimmerman MD, Eum S, Sarathy J, O'Brien P, Chen C, Kaya F, Weiner DM, Chen P-Y, Song T, Lee M, Shim TS, Cho JS, Kim W, Cho SN, Olivier KN, Barry CE, Dartois V. 2015. The association between sterilizing activity and drug distribution into tuberculosis lesions. Nat Med 21:1223–1227. https://doi.org/10.1038/nm.3937.
16. Dartois V. 2014. The path of anti-tuberculosis drugs: from blood to lesions to mycobacterial cells. Nat Rev Microbiol 12:159–167. https://doi.org/10.1038/nrmicro3200.
17. Dartois V, Barry CE, III. 2013. A medicinal chemists' guide to the unique difficulties of lead optimization for tuberculosis. Bioorg Med Chem Lett 23:4741–4750. https://doi.org/10.1016/j.bmcl.2013.07.006.
18. Guerrini V, Gennaro ML. 2019. Foam cells: one size doesn't fit all. Trends Immunol 40:1163–1179. https://doi.org/10.1016/j.it.2019.10.002.
19. Hunter RL. 2016. Tuberculosis as a three-act play: a new paradigm for the pathogenesis of pulmonary tuberculosis. Tuberculosis (Edinb) 97:8–17. https://doi.org/10.1016/j.tube.2015.11.010.
20. Hunter RL, Jagannath C, Actor JK. 2007. Pathology of postprimary tuberculosis in humans and mice: contradiction of long-held beliefs. Tuberculosis (Edinb) 87:267–278. https://doi.org/10.1016/j.tube.2006.11.003.
21. Dannenberg AM, Jr. 2006. Pathogenesis of human pulmonary tuberculosis: insights from the rabbit model, p 97–119. ASM Press, Washington, DC.
22. Kim MJ, Wainwright HC, Locketz M, Bekker LG, Walther GB, Dittrich C, Visser A, Wang W, Hsu FF, Wiehart U, Tsenova L, Kaplan G, Russell DG. 2010. Caseation of human tuberculosis granulomas correlates with elevated host lipid metabolism. EMBO Mol Med 2:258–274. https://doi.org/10.1002/emmm.201000079.
23. Peyron P, Vaubourgeix J, Poquet Y, Levillain F, Botanch C, Bardou F, Daffe M, Emile JF, Marchou B, Cardona PJ, de Chastellier C, Altare F. 2008. Foamy macrophages from tuberculous patients' granulomas constitute a nutrient-rich reservoir for M. tuberculosis persistence. PLoS Pathog 4:e1000204. https://doi.org/10.1371/journal.ppat.1000204.
24. Laennec R. 1821. A treatise on the diseases of the chest: in which they are described according to their anatomical characters, and their diagnosis established on a new principle by means of acoustick instruments. T&G Underwood, London, England.
25. Guerrini V, Prideaux B, Blanc L, Bruiners N, Arrigucci R, Singh S, Ho-Liang HP, Salamon H, Chen P-Y, Lakehal K, Subbian S, O'Brien P, Via LE, Barry CE, Dartois V, Gennaro ML. 2018. Storage lipid studies in tuberculosis reveal that foam cell biogenesis is disease-specific. PLoS Pathog 14:e1007223. https://doi.org/10.1371/journal.ppat.1007223.
26. Dkhar HK, Nanduri R, Mahajan S, Dave S, Saini A, Somavarapu AK, Arora A, Parkesh R, Thakur KG, Mayilraj S, Gupta P. 2014. Mycobacterium tuberculosis keto-mycolic acid and macrophage nuclear receptor TR4 modulate foamy biogenesis in granulomas: a case of a heterologous and noncanonical ligand-receptor pair. J Immunol 193:295–305. https://doi.org/10.4049/jimmunol.1400092.
27. Bowdish DM, Sakamoto K, Kim MJ, Kroos M, Mukhopadhyay S, Leifer CA, Tryggvason K, Gordon S, Russell DG. 2009. MARCO, TLR2, and CD14 are required for macrophage cytokine responses to mycobacterial trehalose dimycolate and Mycobacterium tuberculosis. PLoS Pathog 5:e1000474. https://doi.org/10.1371/journal.ppat.1000474.
28. Bostrom P, Magnusson B, Svensson PA, Wiklund O, Boren J, Carlsson LM, Stahlman M, Olofsson SO, Hulten LM. 2006. Hypoxia converts human macrophages into triglyceride-loaded foam cells. Arterioscler Thromb Vasc Biol 26:1871–1876. https://doi.org/10.1161/01.ATV.0000229665.78997.0b.
29. Milosavljevic D, Kontush A, Griglio S, Le Naour G, Thillet J, Chapman MJ. 2003. VLDL-induced triglyceride accumulation in human macrophages is mediated by modulation of LPL lipolytic activity in the absence of change in LPL mass. Biochim Biophys Acta 1631:51–60. https://doi.org/10.1016/s1388-1981(02)00355-4.
30. den Hartigh LJ, Connolly-Rohrbach JE, Fore S, Huser TR, Rutledge JC. 2010. Fatty acids from very low-density lipoprotein lipolysis products induce lipid droplet accumulation in human monocytes. J Immunol 184:3927–3936. https://doi.org/10.4049/jimmunol.0903475.

31. Ouimet M, Koster S, Sakowski E, Ramkhelawon B, van Solingen C, Oldebeken S, Karunakaran D, Portal-Celhay C, Sheedy FJ, Ray TD, Cecchini K, Zamore PD, Rayner KJ, Marcel YL, Philips JA, Moore KJ. 2016. Mycobacterium tuberculosis induces the miR-33 locus to reprogram autophagy and host lipid metabolism. Nat Immunol 17:677–686. https://doi.org/10.1038/ni.3434.
32. Leong FJ, Dartois V, Dick T. 2011. A color atlas of comparative pathology of pulmonary tuberculosis. CRC Press, Singapore.
33. Grosset J. 2003. Mycobacterium tuberculosis in the extracellular compartment: an underestimated adversary. Antimicrob Agents Chemother 47:833–836. https://doi.org/10.1128/aac.47.3.833-836.2003.
34. Ernst JD. 2012. The immunological life cycle of tuberculosis. Nat Rev Immunol 12:581–591. https://doi.org/10.1038/nri3259.
35. Kwan CK, Ernst JD. 2011. HIV and tuberculosis: a deadly human syndemic. Clin Microbiol Rev 24:351–376. https://doi.org/10.1128/CMR.00042-10.
36. Russell DG, VanderVen BC, Lee W, Abramovitch RB, Kim MJ, Homolka S, Niemann S, Rohde KH. 2010. Mycobacterium tuberculosis wears what it eats. Cell Host Microbe 8:68–76. https://doi.org/10.1016/j.chom.2010.06.002.
37. Kroon EE, Coussens AK, Kinnear C, Orlova M, Moller M, Seeger A, Wilkinson RJ, Hoal EG, Schurr E. 2018. Neutrophils: innate effectors of TB resistance? Front Immunol 9:2637. https://doi.org/10.3389/fimmu.2018.02637.
38. Lowe DM, Redford PS, Wilkinson RJ, O'Garra A, Martineau AR. 2012. Neutrophils in tuberculosis: friend or foe? Trends Immunol 33:14–25. https://doi.org/10.1016/j.it.2011.10.003.
39. Cardona PJ. 2015. The key role of exudative lesions and their encapsulation: lessons learned from the pathology of human pulmonary tuberculosis. Front Microbiol 6:612. https://doi.org/10.3389/fmicb.2015.00612.
40. Mattila JT, Ojo OO, Kepka-Lenhart D, Marino S, Kim JH, Eum SY, Via LE, Barry CE, III, Klein E, Kirschner DE, Morris SM, Jr, Lin PL, Flynn JL. 2013. Microenvironments in tuberculous granulomas are delineated by distinct populations of macrophage subsets and expression of nitric oxide synthase and arginase isoforms. J Immunol 191:773–784. https://doi.org/10.4049/jimmunol.1300113.
41. Lowe DM, Demaret J, Bangani N, Nakiwala JK, Goliath R, Wilkinson KA, Wilkinson RJ, Martineau AR. 2018. Differential effect of viable versus necrotic neutrophils on Mycobacterium tuberculosis growth and cytokine induction in whole blood. Front Immunol 9:903. https://doi.org/10.3389/fimmu.2018.00903.
42. Eum SY, Kong JH, Hong MS, Lee YJ, Kim JH, Hwang SH, Cho SN, Via LE, Barry CE, III. 2010. Neutrophils are the predominant infected phagocytic cells in the airways of patients with active pulmonary TB. Chest 137:122–128. https://doi.org/10.1378/chest.09-0903.
43. Mishra BB, Lovewell RR, Olive AJ, Zhang G, Wang W, Eugenin E, Smith CM, Phuah JY, Long JE, Dubuke ML, Palace SG, Goguen JD, Baker RE, Nambi S, Mishra R, Booty MG, Baer CE, Shaffer SA, Dartois V, McCormick BA, Chen X, Sassetti CM. 2017. Nitric oxide prevents a pathogen-permissive granulocytic inflammation during tuberculosis. Nat Microbiol 2:17072. https://doi.org/10.1038/nmicrobiol.2017.72.
44. Marzo E, Vilaplana C, Tapia G, Diaz J, Garcia V, Cardona PJ. 2014. Damaging role of neutrophilic infiltration in a mouse model of progressive tuberculosis. Tuberculosis (Edinb) 94:55–64. https://doi.org/10.1016/j.tube.2013.09.004.
45. Canetti G. 1955. The tubercle bacillus in the pulmonary lesion of man. Springer Publishing Company, New York, NY.
46. Cardona PJ. 2011. A spotlight on liquefaction: evidence from clinical settings and experimental models in tuberculosis. Clin Dev Immunol 2011:868246. https://doi.org/10.1155/2011/868246.
47. Chang KC, Leung CC, Yew WW, Ho SC, Tam CM. 2004. A nested case-control study on treatment-related risk factors for early relapse of tuberculosis. Am J Respir Crit Care Med 170:1124–1130. https://doi.org/10.1164/rccm.200407-905OC.
48. Chang KC, Leung CC, Yew WW, Chan SL, Tam CM. 2006. Dosing schedules of 6-month regimens and relapse for pulmonary tuberculosis. Am J Respir Crit Care Med 174:1153–1158. https://doi.org/10.1164/rccm.200605-637OC.
49. Nardell EA, Piessens WF. 2000. Transmission of tuberculosis, p 215–240. *In* Reichman LB, Hershfield ES (ed), Tuberculosis: a comprehensive international approach. Marcel Dekker, New York, NY.
50. Imperial MZ, Nahid P, Phillips PPJ, Davies GR, Fielding K, Hanna D, Hermann D, Wallis RS, Johnson JL, Lienhardt C, Savic RM. 2018. A patient-level pooled analysis of treatment-shortening regimens for drug-susceptible pulmonary tuberculosis. Nat Med 24:1708–1715. https://doi.org/10.1038/s41591-018-0224-2.
51. Blanc L, Lenaerts A, Dartois V, Prideaux B. 2018. Visualization of mycobacterial biomarkers and tuberculosis drugs in infected tissue by MALDI-MS imaging. Anal Chem 90:6275–6282. https://doi.org/10.1021/acs.analchem.8b00985.
52. Ahmad Z, Fraig MM, Bisson GP, Nuermberger EL, Grosset JH, Karakousis PC. 2011. Dose-dependent activity of pyrazinamide in animal models of intracellular and extracellular tuberculosis infections. Antimicrob Agents Chemother 55:1527–1532. https://doi.org/10.1128/AAC.01524-10.
53. Irwin SM, Driver E, Lyon E, Schrupp C, Ryan G, Gonzalez-Juarrero M, Basaraba RJ, Nuermberger EL, Lenaerts AJ. 2015. Presence of multiple lesion types with vastly different microenvironments in C3HeB/FeJ mice following aerosol infection with Mycobacterium tuberculosis. Dis Model Mech 8:591–602. https://doi.org/10.1242/dmm.019570.
54. Vilcheze C, Kremer L. 2017. Acid-fast positive and acid-fast negative Mycobacterium tuberculosis: the Koch paradox. Microbiol Spectr 5:TBTB2-0003-2015. https://doi.org/10.1128/microbiolspec.TBTB2-0003-2015.
55. Seiler P, Ulrichs T, Bandermann S, Pradl L, Jorg S, Krenn V, Morawietz L, Kaufmann SH, Aichele P. 2003. Cell-wall alterations as an attribute of Mycobacterium tuberculosis in latent infection. J Infect Dis 188:1326–1331. https://doi.org/10.1086/378563.
56. Ulrichs T, Kaufmann SH. 2006. New insights into the function of granulomas in human tuberculosis. J Pathol 208:261–269. https://doi.org/10.1002/path.1906.
57. Samanovic MI, Hsu HC, Jones MB, Jones V, McNeil MR, Becker SH, Jordan AT, Strnad M, Xu C, Jackson M, Li H, Darwin KH. 2018. Cytokinin signaling in Mycobacterium tuberculosis. mBio 9:e00989-18. https://doi.org/10.1128/mBio.00989-18.
58. Subbian S, Eugenin E, Kaplan G. 2014. Detection of Mycobacterium tuberculosis in latently infected lungs by immunohistochemistry and confocal microscopy. J Med Microbiol 63:1432–1435. https://doi.org/10.1099/jmm.0.081091-0.
59. Ryan GJ, Shapiro HM, Lenaerts AJ. 2014. Improving acid-fast fluorescent staining for the detection of mycobacteria using a new nucleic acid staining approach. Tuberculosis (Edinb) 94:511–518. https://doi.org/10.1016/j.tube.2014.07.004.
60. Canetti G. 1965. Present aspects of bacterial resistance in tuberculosis. Am Rev Respir Dis 92:687–703.
61. Dartois V, Saito K, Warrier T, Nathan C. 2016. New evidence for the complexity of the population structure of Mycobacterium tuberculosis increases the diagnostic and biologic challenges. Am J Respir Crit Care Med 194:1448–1451. https://doi.org/10.1164/rccm.201607-1431ED.
62. Chengalroyen MD, Beukes GM, Gordhan BG, Streicher EM, Churchyard G, Hafner R, Warren R, Otwombe K, Martinson N, Kana BD. 2016. Detection and quantification of differentially culturable tubercle bacteria in sputum from patients with tuberculosis. Am J Respir Crit Care Med 194:1532–1540. https://doi.org/10.1164/rccm.201604-0769OC.
63. Turapov O, O'Connor BD, Sarybaeva AA, Williams C, Patel H, Kadyrov AS, Sarybaev AS, Woltmann G, Barer MR, Mukamolova GV. 2016. Phenotypically adapted Mycobacterium tuberculosis populations from sputum are tolerant to first-line drugs. Antimicrob Agents Chemother 60:2476–2483. https://doi.org/10.1128/AAC.01380-15.
64. Mukamolova GV, Turapov O, Malkin J, Woltmann G, Barer MR. 2010. Resuscitation-promoting factors reveal an occult population of tubercle bacilli in sputum. Am J Respir Crit Care Med 181:174–180. https://doi.org/10.1164/rccm.200905-0661OC.
65. Wayne LG, Hayes LG. 1996. An in vitro model for sequential study of shiftdown of Mycobacterium tuberculosis through two stages of nonreplicating persistence. Infect Immun 64:2062–2069. https://doi.org/10.1128/IAI.64.6.2062-2069.1996.
66. Dick T, Lee BH, Murugasu-Oei B. 1998. Oxygen depletion induced dormancy in Mycobacterium smegmatis. FEMS Microbiol Lett 163:159–164. https://doi.org/10.1111/j.1574-6968.1998.tb13040.x.
67. Lim A, Eleuterio M, Hutter B, Murugasu-Oei B, Dick T. 1999. Oxygen depletion-induced dormancy in Mycobacterium bovis BCG. J Bacteriol 181:2252–2256. https://doi.org/10.1128/JB.181.7.2252-2256.1999.
68. Nathan C, Shiloh MU. 2000. Reactive oxygen and nitrogen intermediates in the relationship between mammalian hosts and microbial pathogens. Proc Natl Acad Sci U S A 97:8841–8848. https://doi.org/10.1073/pnas.97.16.8841.

69. Nathan C, Ehrt S. 2004. Tuberculosis, p 215–235. Lippincott Williams & Wilkins, Philadelphia, PA.
70. Loebel RO, Shorr E, Richardson HB. 1933. The influence of adverse conditions upon the respiratory metabolism and growth of human tubercle bacilli. J Bacteriol 26:167–200. https://doi.org/10.1128/JB.26.2.167-200.1933.
71. Baker JJ, Johnson BK, Abramovitch RB. 2014. Slow growth of Mycobacterium tuberculosis at acidic pH is regulated by phoPR and host-associated carbon sources. Mol Microbiol 94:56–69. https://doi.org/10.1111/mmi.12688.
72. Gold B, Warrier T, Nathan C. 2015. A multi-stress model for high throughput screening against non-replicating Mycobacterium tuberculosis. Methods Mol Biol 1285:293–315. https://doi.org/10.1007/978-1-4939-2450-9_18.
73. Munoz-Elias EJ, Timm J, Botha T, Chan WT, Gomez JE, McKinney JD. 2005. Replication dynamics of Mycobacterium tuberculosis in chronically infected mice. Infect Immun 73:546–551. https://doi.org/10.1128/IAI.73.1.546-551.2005.
74. Burdon KL. 1946. Disparity in appearance of true Hansen's bacilli and cultured leprosy bacilli when stained for fat. J Bacteriol 52:679–680. https://doi.org/10.1128/JB.52.6.679-680.1946.
75. Christensen H, Garton NJ, Horobin RW, Minnikin DE, Barer MR. 1999. Lipid domains of mycobacteria studied with fluorescent molecular probes. Mol Microbiol 31:1561–1572. https://doi.org/10.1046/j.1365-2958.1999.01304.x.
76. Garton NJ, Christensen H, Minnikin DE, Adegbola RA, Barer MR. 2002. Intracellular lipophilic inclusions of mycobacteria in vitro and in sputum. Microbiology 148:2951–2958. https://doi.org/10.1099/00221287-148-10-2951.
77. Garton NJ, Waddell SJ, Sherratt AL, Lee SM, Smith RJ, Senner C, Hinds J, Rajakumar K, Adegbola RA, Besra GS, Butcher PD, Barer MR. 2008. Cytological and transcript analyses reveal fat and lazy persister-like bacilli in tuberculous sputum. PLoS Med 5:e75. https://doi.org/10.1371/journal.pmed.0050075.
78. Vijay S, Hai HT, Thu DDA, Johnson E, Pielach A, Phu NH, Thwaites GE, Thuong N. 2017. Ultrastructural analysis of cell envelope and accumulation of lipid inclusions in clinical Mycobacterium tuberculosis isolates from sputum, oxidative stress, and iron deficiency. Front Microbiol 8:2681. https://doi.org/10.3389/fmicb.2017.02681.
79. Deb C, Lee CM, Dubey VS, Daniel J, Abomoelak B, Sirakova TD, Pawar S, Rogers L, Kolattukudy PE. 2009. A novel in vitro multiple-stress dormancy model for Mycobacterium tuberculosis generates a lipid-loaded, drug-tolerant, dormant pathogen. PLoS One 4:e6077. https://doi.org/10.1371/journal.pone.0006077.
80. Daniel J, Maamar H, Deb C, Sirakova TD, Kolattukudy PE. 2011. Mycobacterium tuberculosis uses host triacylglycerol to accumulate lipid droplets and acquires a dormancy-like phenotype in lipid-loaded macrophages. PLoS Pathog 7:e1002093. https://doi.org/10.1371/journal.ppat.1002093.
81. Kapoor N, Pawar S, Sirakova TD, Deb C, Warren WL, Kolattukudy PE. 2013. Human granuloma in vitro model, for TB dormancy and resuscitation. PLoS One 8:e53657. https://doi.org/10.1371/journal.pone.0053657.
82. Daniel J, Kapoor N, Sirakova T, Sinha R, Kolattukudy P. 2016. The perilipin-like PPE15 protein in Mycobacterium tuberculosis is required for triacylglycerol accumulation under dormancy-inducing conditions. Mol Microbiol 101:784–794. https://doi.org/10.1111/mmi.13422.
83. Alvarez HM, Steinbuchel A. 2002. Triacylglycerols in prokaryotic microorganisms. Appl Microbiol Biotechnol 60:367–376. https://doi.org/10.1007/s00253-002-1135-0.
84. Daniel J, Deb C, Dubey VS, Sirakova TD, Abomoelak B, Morbidoni HR, Kolattukudy PE. 2004. Induction of a novel class of diacylglycerol acyltransferases and triacylglycerol accumulation in Mycobacterium tuberculosis as it goes into a dormancy-like state in culture. J Bacteriol 186:5017–5030. https://doi.org/10.1128/JB.186.15.5017-5030.2004.
85. Caire-Brandli I, Papadopoulos A, Malaga W, Marais D, Canaan S, Thilo L, de Chastellier C. 2014. Reversible lipid accumulation and associated division arrest of Mycobacterium avium in lipoprotein-induced foamy macrophages may resemble key events during latency and reactivation of tuberculosis. Infect Immun 82:476–490. https://doi.org/10.1128/IAI.01196-13.
86. Sirakova TD, Dubey VS, Deb C, Daniel J, Korotkova TA, Abomoelak B, Kolattukudy PE. 2006. Identification of a diacylglycerol acyltransferase gene involved in accumulation of triacylglycerol in Mycobacterium tuberculosis under stress. Microbiology 152:2717–2725. https://doi.org/10.1099/mic.0.28993-0.
87. Park HD, Guinn KM, Harrell MI, Liao R, Voskuil MI, Tompa M, Schoolnik GK, Sherman DR. 2003. Rv3133c/dosR is a transcription factor that mediates the hypoxic response of Mycobacterium tuberculosis. Mol Microbiol 48:833–843. https://doi.org/10.1046/j.1365-2958.2003.03474.x.
88. Maurya RK, Bharti S, Krishnan MY. 2018. Triacylglycerols: fuelling the hibernating Mycobacterium tuberculosis. Front Cell Infect Microbiol 8:450. https://doi.org/10.3389/fcimb.2018.00450.
89. Armstrong RM, Adams KL, Zilisch JE, Bretl DJ, Sato H, Anderson DM, Zahrt TC. 2016. Rv2744c is a PspA ortholog that regulates lipid droplet homeostasis and nonreplicating persistence in Mycobacterium tuberculosis. J Bacteriol 198:1645–1661. https://doi.org/10.1128/JB.01001-15.
90. Deb C, Daniel J, Sirakova TD, Abomoelak B, Dubey VS, Kolattukudy PE. 2006. A novel lipase belonging to the hormone-sensitive lipase family induced under starvation to utilize stored triacylglycerol in Mycobacterium tuberculosis. J Biol Chem 281:3866–3875. https://doi.org/10.1074/jbc.M505556200.
91. Pacl HT, Reddy VP, Saini V, Chinta KC, Steyn A. 2018. Host-pathogen redox dynamics modulate Mycobacterium tuberculosis pathogenesis. Pathog Dis 76:fty036. https://doi.org/10.1093/femspd/fty036.
92. Reed MB, Gagneux S, Deriemer K, Small PM, Barry CE, III. 2007. The W-Beijing lineage of Mycobacterium tuberculosis overproduces triglycerides and has the DosR dormancy regulon constitutively upregulated. J Bacteriol 189:2583–2589. https://doi.org/10.1128/JB.01670-06.
93. Barisch C, Soldati T. 2017. Mycobacterium marinum degrades both triacylglycerols and phospholipids from its dictyostelium host to synthesise its own triacylglycerols and generate lipid inclusions. PLoS Pathog 13:e1006095. https://doi.org/10.1371/journal.ppat.1006095.
94. Bouzid F, Bregeon F, Poncin I, Weber P, Drancourt M, Canaan S. 2017. Mycobacterium canettii infection of adipose tissues. Front Cell Infect Microbiol 7:189. https://doi.org/10.3389/fcimb.2017.00189.
95. Loebel RO, Shorr E, Richardson HB. 1933. The influence of foodstuffs upon the respiratory metabolism and growth of human tubercle bacilli. J Bacteriol 26:139–166. https://doi.org/10.1128/JB.26.2.139-166.1933.
96. Piddington DL, Kashkouli A, Buchmeier NA. 2000. Growth of Mycobacterium tuberculosis in a defined medium is very restricted by acid pH and Mg(2+) levels. Infect Immun 68:4518–4522. https://doi.org/10.1128/iai.68.8.4518-4522.2000.
97. Abramovitch RB, Rohde KH, Hsu FF, Russell DG. 2011. aprABC: a Mycobacterium tuberculosis complex-specific locus that modulates pH-driven adaptation to the macrophage phagosome. Mol Microbiol 80:678–694. https://doi.org/10.1111/j.1365-2958.2011.07601.x.
98. Zhang Y, Scorpio A, Nikaido H, Sun Z. 1999. Role of acid pH and deficient efflux of pyrazinoic acid in unique susceptibility of Mycobacterium tuberculosis to pyrazinamide. J Bacteriol 181:2044–2049. https://doi.org/10.1128/JB.181.7.2044-2049.1999.
99. Vandal OH, Pierini LM, Schnappinger D, Nathan CF, Ehrt S. 2008. A membrane protein preserves intrabacterial pH in intraphagosomal Mycobacterium tuberculosis. Nat Med 14:849–854. https://doi.org/10.1038/nm.1795.
100. Salfinger M, Heifets LB. 1988. Determination of pyrazinamide MICs for Mycobacterium tuberculosis at different pHs by the radiometric method. Antimicrob Agents Chemother 32:1002–1004. https://doi.org/10.1128/aac.32.7.1002.
101. McDermott W, Tompsett R. 1954. Activation of pyrazinamide and nicotinamide in acidic environments in vitro. Am Rev Tuberc 70:748–754.
102. Weiss C, Tabachnick J, Cohen HP. 1954. Mechanism of softening of tubercles. III. Hydrolysis of protein and nucleic acid during anaerobic autolysis of normal and tuberculous lung tissue in vitro. AMA Arch Pathol 57:179–193.
103. Kempker RR, Heinrichs MT, Nikolaishvili K, Sabulua I, Bablishvili N, Gogishvili S, Avaliani Z, Tukvadze N, Little B, Bernheim A, Read TD, Guarner J, Derendorf H, Peloquin CA, Blumberg HM, Vashakidze S. 2017. Lung tissue concentrations of pyrazinamide among patients with drug-resistant pulmonary tuberculosis. Antimicrob Agents Chemother 61:e00226-17. https://doi.org/10.1128/AAC.00226-17.
104. Koller F, Leuthardt F. 1934. Nekrose und Autolyse. Beitrag zur Kenntnis der Dystrophischen Verkalkung. Klin Wochenschr 43:1527–1529. https://doi.org/10.1007/BF01779121.
105. Dahl HK. 1950. Examination of pH in tuberculous pus. Acta Orthop Scand 20:176–180. https://doi.org/10.3109/17453675009043416.
106. MacMicking JD, Taylor GA, McKinney JD. 2003. Immune control of

tuberculosis by IFN-gamma-inducible LRG-47. Science 302:654–659. https://doi.org/10.1126/science.1088063.
107. Pethe K, Swenson DL, Alonso S, Anderson J, Wang C, Russell DG. 2004. Isolation of Mycobacterium tuberculosis mutants defective in the arrest of phagosome maturation. Proc Natl Acad Sci U S A 101:13642–13647. https://doi.org/10.1073/pnas.0401657101.
108. Sturgill-Koszycki S, Schlesinger PH, Chakraborty P, Haddix PL, Collins HL, Fok AK, Allen RD, Gluck SL, Heuser J, Russell DG. 1994. Lack of acidification in Mycobacterium phagosomes produced by exclusion of the vesicular proton-ATPase. Science 263:678–681. https://doi.org/10.1126/science.8303277.
109. Tsai MC, Chakravarty S, Zhu G, Xu J, Tanaka K, Koch C, Tufariello J, Flynn J, Chan J. 2006. Characterization of the tuberculous granuloma in murine and human lungs: cellular composition and relative tissue oxygen tension. Cell Microbiol 8:218–232. https://doi.org/10.1111/j.1462-5822.2005.00612.x.
110. Aguilera KY, Brekken RA. 2014. Hypoxia studies with pimonidazole in vivo. Bio Protoc 4:e1254.
111. Via LE, Lin PL, Ray SM, Carrillo J, Allen SS, Eum SY, Taylor K, Klein E, Manjunatha U, Gonzales J, Lee EG, Park SK, Raleigh JA, Cho SN, McMurray DN, Flynn JL, Barry CE, III. 2008. Tuberculous granulomas are hypoxic in guinea pigs, rabbits, and non-human primates. Infect Immun 76:2333–2340. https://doi.org/10.1128/IAI.01515-07.
112. Haapanen JH, Kass I, Gensini G, Middlebrook G. 1959. Studies on the gaseous content of tuberculous cavities. Am Rev Respir Dis 80:1–5.
113. Belton M, Brilha S, Manavaki R, Mauri F, Nijran K, Hong YT, Patel NH, Dembek M, Tezera L, Green J, Moores R, Aigbirhio F, Al-Nahhas A, Fryer TD, Elkington PT, Friedland JS. 2016. Hypoxia and tissue destruction in pulmonary TB. Thorax 71:1145–1153. https://doi.org/10.1136/thoraxjnl-2015-207402.
114. Nuermberger E. 2008. Using animal models to develop new treatments for tuberculosis. Semin Respir Crit Care Med 29:542–551. https://doi.org/10.1055/s-0028-1085705.
115. Aly S, Wagner K, Keller C, Malm S, Malzan A, Brandau S, Bange FC, Ehlers S. 2006. Oxygen status of lung granulomas in Mycobacterium tuberculosis-infected mice. J Pathol 210:298–305. https://doi.org/10.1002/path.2055.
116. Wayne LG. 2001. In vitro model of hypoxically induced nonreplicating persistence of Mycobacterium tuberculosis. Methods Mol Med 54:247–269. https://doi.org/10.1385/1-59259-147-7:247.
117. Rao SP, Alonso S, Rand L, Dick T, Pethe K. 2008. The protonmotive force is required for maintaining ATP homeostasis and viability of hypoxic, nonreplicating Mycobacterium tuberculosis. Proc Natl Acad Sci U S A 105:11945–11950. https://doi.org/10.1073/pnas.0711697105.
118. Sherman DR, Voskuil M, Schnappinger D, Liao R, Harrell MI, Schoolnik GK. 2001. Regulation of the Mycobacterium tuberculosis hypoxic response gene encoding alpha-crystallin. Proc Natl Acad Sci U S A 98:7534–7539. https://doi.org/10.1073/pnas.121172498.
119. Lakshminarayana SB, Huat TB, Ho PC, Manjunatha UH, Dartois V, Dick T, Rao SP. 2015. Comprehensive physicochemical, pharmacokinetic and activity profiling of anti-TB agents. J Antimicrob Chemother 70:857–867. https://doi.org/10.1093/jac/dku457.
120. Liu Z, Gao Y, Yang H, Bao H, Qin L, Zhu C, Chen Y, Hu Z. 2016. Impact of hypoxia on drug resistance and growth characteristics of Mycobacterium tuberculosis clinical isolates. PLoS One 11:e0166052. https://doi.org/10.1371/journal.pone.0166052.
121. Leistikow RL, Morton RA, Bartek IL, Frimpong I, Wagner K, Voskuil MI. 2010. The Mycobacterium tuberculosis DosR regulon assists in metabolic homeostasis and enables rapid recovery from nonrespiring dormancy. J Bacteriol 192:1662–1670. https://doi.org/10.1128/JB.00926-09.
122. Hudock TA, Foreman TW, Bandyopadhyay N, Gautam US, Veatch AV, LoBato DN, Gentry KM, Golden NA, Cavigli A, Mueller M, Hwang SA, Hunter RL, Alvarez X, Lackner AA, Bader JS, Mehra S, Kaushal D. 2017. Hypoxia sensing and persistence genes are expressed during the intragranulomatous survival of Mycobacterium tuberculosis. Am J Respir Cell Mol Biol 56:637–647. https://doi.org/10.1165/rcmb.2016-0239OC.
123. Subbian S, Tsenova L, Yang G, O'Brien P, Parsons S, Peixoto B, Taylor L, Fallows D, Kaplan G. 2011. Chronic pulmonary cavitary tuberculosis in rabbits: a failed host immune response. Open Biol 1:110016. https://doi.org/10.1098/rsob.110016.
124. Ramos L, Obregon-Henao A, Henao-Tamayo M, Bowen R, Lunney JK, Gonzalez-Juarrero M. 2017. The minipig as an animal model to study Mycobacterium tuberculosis infection and natural transmission. Tuberculosis (Edinb) 106:91–98. https://doi.org/10.1016/j.tube.2017.07.003.
125. Neyrolles O, Wolschendorf F, Mitra A, Niederweis M. 2015. Mycobacteria, metals, and the macrophage. Immunol Rev 264:249–263. https://doi.org/10.1111/imr.12265.
126. Marcela Rodriguez G, Neyrolles O. 2014. Metallobiology of tuberculosis. Microbiol Spectr 2:MGM2-0012-2013. https://doi.org/10.1128/microbiolspec.MGM2-0012-2013.
127. Kurthkoti K, Amin H, Marakalala MJ, Ghanny S, Subbian S, Sakatos A, Livny J, Fortune SM, Berney M, Rodriguez GM. 2017. The capacity of Mycobacterium tuberculosis to survive iron starvation might enable it to persist in iron-deprived microenvironments of human granulomas. mBio 8:e01092-17. https://doi.org/10.1128/mBio.01092-17.
128. Wells RM, Jones CM, Xi Z, Speer A, Danilchanka O, Doornbos KS, Sun P, Wu F, Tian C, Niederweis M. 2013. Discovery of a siderophore export system essential for virulence of Mycobacterium tuberculosis. PLoS Pathog 9:e1003120. https://doi.org/10.1371/journal.ppat.1003120.
129. Reddy PV, Puri RV, Chauhan P, Kar R, Rohilla A, Khera A, Tyagi AK. 2013. Disruption of mycobactin biosynthesis leads to attenuation of Mycobacterium tuberculosis for growth and virulence. J Infect Dis 208:1255–1265. https://doi.org/10.1093/infdis/jit250.
130. Rodriguez GM, Voskuil MI, Gold B, Schoolnik GK, Smith I. 2002. *ideR*, an essential gene in *Mycobacterium tuberculosis*: role of IdeR in iron-dependent gene expression, iron metabolism, and oxidative stress response. Infect Immun 70:3371–3381. https://doi.org/10.1128/iai.70.7.3371-3381.2002.
131. Gordeuk VR, McLaren CE, MacPhail AP, Deichsel G, Bothwell TH. 1996. Associations of iron overload in Africa with hepatocellular carcinoma and tuberculosis: Strachan's 1929 thesis revisited. Blood 87:3470–3476. https://doi.org/10.1182/blood.V87.8.3470.bloodjournal8783470.
132. Gangaidzo IT, Moyo VM, Mvundura E, Aggrey G, Murphree NL, Khumalo H, Saungweme T, Kasvosve I, Gomo ZA, Rouault T, Boelaert JR, Gordeuk VR. 2001. Association of pulmonary tuberculosis with increased dietary iron. J Infect Dis 184:936–939. https://doi.org/10.1086/323203.
133. Murray MJ, Murray AB, Murray MB, Murray CJ. 1978. The adverse effect of iron repletion on the course of certain infections. Br Med J 2:1113–1115. https://doi.org/10.1136/bmj.2.6145.1113.
134. Boelaert JR, Vandecasteele SJ, Appelberg R, Gordeuk VR. 2007. The effect of the host's iron status on tuberculosis. J Infect Dis 195:1745–1753. https://doi.org/10.1086/518040.
135. Marakalala MJ, Raju RM, Sharma K, Zhang YJ, Eugenin EA, Prideaux B, Daudelin IB, Chen PY, Booty MG, Kim JH, Eum SY, Via LE, Behar SM, Barry CE, III, Mann M, Dartois V, Rubin EJ. 2016. Inflammatory signaling in human tuberculosis granulomas is spatially organized. Nat Med 22:531–538. https://doi.org/10.1038/nm.4073.
136. Nandy A, Mondal AK, Pandey R, Arumugam P, Dawa S, Jaisinghani N, Rao V, Dash D, Gandotra S. 2018. Adipocyte model of Mycobacterium tuberculosis infection reveals differential availability of iron to bacilli in the lipid-rich caseous environment. Infect Immun 86:e00041-18. https://doi.org/10.1128/IAI.00041-18.
137. Gengenbacher M, Rao SP, Pethe K, Dick T. 2010. Nutrient-starved, non-replicating Mycobacterium tuberculosis requires respiration, ATP synthase and isocitrate lyase for maintenance of ATP homeostasis and viability. Microbiology 156:81–87. https://doi.org/10.1099/mic.0.033084-0.
138. Betts JC, Lukey PT, Robb LC, McAdam RA, Duncan K. 2002. Evaluation of a nutrient starvation model of Mycobacterium tuberculosis persistence by gene and protein expression profiling. Mol Microbiol 43:717–731. https://doi.org/10.1046/j.1365-2958.2002.02779.x.
139. Sarathy J, Dartois V, Dick T, Gengenbacher M. 2013. Reduced drug uptake in phenotypically resistant nutrient-starved nonreplicating Mycobacterium tuberculosis. Antimicrob Agents Chemother 57:1648–1653. https://doi.org/10.1128/AAC.02202-12.
140. Cole ST, Brosch R, Parkhill J, Garnier T, Churcher C, Harris D, Gordon SV, Eiglmeier K, Gas S, Barry CE, III, Tekaia F, Badcock K, Basham D, Brown D, Chillingworth T, Connor R, Davies R, Devlin K, Feltwell T, Gentles S, Hamlin N, Holroyd S, Hornsby T, Jagels K, Krogh A, McLean J, Moule S, Murphy L, Oliver K, Osborne J, Quail MA, Rajandream MA, Rogers J, Rutter S, Seeger K, Skelton J, Squares R, Squares S, Sulston JE, Taylor K, Whitehead S, Barrell BG. 1998. Deciphering the biology of Mycobacterium tuberculosis from the complete genome sequence. Nature 393:537–544. https://doi.org/10.1038/31159.
141. Russell DG, Cardona PJ, Kim MJ, Allain S, Altare F. 2009. Foamy macrophages and the progression of the human tuberculosis granuloma. Nat Immunol 10:943–948. https://doi.org/10.1038/ni.1781.
142. Munoz-Elias EJ, Upton AM, Cherian J, McKinney JD. 2006. Role of the

methylcitrate cycle in Mycobacterium tuberculosis metabolism, intracellular growth, and virulence. Mol Microbiol 60:1109–1122. https://doi.org/10.1111/j.1365-2958.2006.05155.x.
143. Pandey AK, Sassetti CM. 2008. Mycobacterial persistence requires the utilization of host cholesterol. Proc Natl Acad Sci U S A 105:4376–4380. https://doi.org/10.1073/pnas.0711159105.
144. Miner MD, Chang JC, Pandey AK, Sassetti CM, Sherman DR. 2009. Role of cholesterol in Mycobacterium tuberculosis infection. Indian J Exp Biol 47:407–411.
145. Brzostek A, Pawelczyk J, Rumijowska-Galewicz A, Dziadek B, Dziadek J. 2009. Mycobacterium tuberculosis is able to accumulate and utilize cholesterol. J Bacteriol 191:6584–6591. https://doi.org/10.1128/JB.00488-09.
146. Schnappinger D, Ehrt S, Voskuil MI, Liu Y, Mangan JA, Monahan IM, Dolganov G, Efron B, Butcher PD, Nathan C, Schoolnik GK. 2003. Transcriptional adaptation of Mycobacterium tuberculosis within macrophages: insights into the phagosomal environment. J Exp Med 198:693–704. https://doi.org/10.1084/jem.20030846.
147. Rohde KH, Veiga DF, Caldwell S, Balazsi G, Russell DG. 2012. Linking the transcriptional profiles and the physiological states of Mycobacterium tuberculosis during an extended intracellular infection. PLoS Pathog 8:e1002769. https://doi.org/10.1371/journal.ppat.1002769.
148. Kaplan G, Post FA, Moreira AL, Wainwright H, Kreiswirth BN, Tanverdi M, Mathema B, Ramaswamy SV, Walther G, Steyn LM, Barry CE, III, Bekker LG. 2003. Mycobacterium tuberculosis growth at the cavity surface: a microenvironment with failed immunity. Infect Immun 71:7099–7108. https://doi.org/10.1128/iai.71.12.7099-7108.2003.
149. Hunter RL, Olsen MR, Jagannath C, Actor JK. 2006. Multiple roles of cord factor in the pathogenesis of primary, secondary, and cavitary tuberculosis, including a revised description of the pathology of secondary disease. Ann Clin Lab Sci 36:371–386.
150. Lanoix JP, Ioerger T, Ormond A, Kaya F, Sacchettini J, Dartois V, Nuermberger E. 2015. Selective inactivity of pyrazinamide against tuberculosis in C3HeB/FeJ mice is best explained by neutral pH of caseum. Antimicrob Agents Chemother 60:735–743. https://doi.org/10.1128/AAC.01370-15.
151. Wayne LG, Sohaskey CD. 2001. Nonreplicating persistence of Mycobacterium tuberculosis. Annu Rev Microbiol 55:139–163. https://doi.org/10.1146/annurev.micro.55.1.139.
152. McKinney JD, Honer zu Bentrup K, Munoz-Elias EJ, Miczak A, Chen B, Chan WT, Swenson D, Sacchettini JC, Jacobs WR, Jr, Russell DG. 2000. Persistence of Mycobacterium tuberculosis in macrophages and mice requires the glyoxylate shunt enzyme isocitrate lyase. Nature 406:735–738. https://doi.org/10.1038/35021074.
153. Mor N, Simon B, Heifets L. 1996. Bacteriostatic and bactericidal activities of benzoxazinorifamycin KRM-1648 against Mycobacterium tuberculosis and Mycobacterium avium in human macrophages. Antimicrob Agents Chemother 40:1482–1485.
154. Lanoix JP, Lenaerts AJ, Nuermberger EL. 2015. Heterogeneous disease progression and treatment response in a C3HeB/FeJ mouse model of tuberculosis. Dis Model Mech 8:603–610. https://doi.org/10.1242/dmm.019513.

Jansy P. Sarathy received her Ph.D. from the National University of Singapore in conjuction with the Novartis Institute for Tropical Diseases. She has since completed a postdoctoral research fellowship at the Public Health Research Institute, Rutgers, NJ, and now works as a Research Assistant Member at the Center for Discovery and Innovation, Hackensack Meridian Health, NJ. She has spent the past 10 years developing *in vitro* assays to facilitate the field of tuberculosis drug discovery. The past few years have been especially focused on exploring the pharmacokinetic and pharmacodynamic interactions of *Mycobacterium tuberculosis* in the caseous core of granulomas.

Véronique Dartois is a Member of the Center for Discovery and Innovation and Professor at the Hackensack School of Medicine. She received her Ph.D. in microbial genetics at the University of Louvain, Belgium. After postdoctoral fellowships at the Scripps Research and Pasteur Institutes, she joined the biotechnology industry in California, with a focus on anti-infective drug discovery. As Executive Director of Pharmacology at the Novartis Institute for Tropical Diseases from 2005 to 2012, she supported drug discovery programs in tuberculosis (TB), dengue fever, and malaria. In 2012, she joined the Public Health Research Institute of Rutgers University to focus on the pharmacological mechanisms contributing to the very long therapy duration required to cure TB and nontuberculous mycobacterial disease. Her team's work has paved to way to rationally build new drug regimens that combine agents with complementary distribution and activity at the complex site of disease, a significant departure from current empirical approaches.